

Traffic signal synchronization

Ding-wei Huang and Wei-neng Huang

Department of Physics, Chung Yuan Christian University, Chung-li, Taiwan

(Received 16 December 2002; published 23 May 2003)

The benefits of traffic signal synchronization are examined within the cellular automata approach. The microsimulations of traffic flow are obtained with different settings of signal period T and time delay δ . Both numerical results and analytical approximations are presented. For undersaturated traffic, the green-light wave solutions can be realized. For saturated traffic, the correlation among the traffic signals has no effect on the throughput. For oversaturated traffic, the benefits of synchronization are manifest only when stochastic noise is suppressed.

DOI: 10.1103/PhysRevE.67.056124

PACS number(s): 89.40.-a, 05.40.-a, 45.70.Vn

I. INTRODUCTION

Transportation simulations are complex and interesting [1]. The numerous details seem to be all linked together and hard to specify microscopically. The probe of underlying dynamics is often started with presumptions on the steady-state collective behavior, which is known to be correct only within certain limits. Thus the low-density dynamics and high-density dynamics are often discussed separately. And the results in the intermediate-density region become quite obscure. A coherent approach applicable to all densities is desired. With recent advances in the cellular automata approaches [2], microsimulations can be taken as virtual reality experiments. With correct street layouts and prescribed driving rules, such microsimulations can be used to explore the hidden dynamics without assuming the equilibrium collective behaviors. In such an approach, macroscopic observables emerge automatically from the microscopic behavior. Similar approaches can be found in statistical physics, where macroscopic phenomena can be obtained from much simplified microscopic models.

The traffic signal is an essential element for managing the transportation network. When the traffic demand is light, the traffic signals usually require no special sequencing. In contrast, when the traffic demand is heavy, the operation of traffic signals requires careful regulation. The benefits of the traffic signal synchronization are widely accepted. With the traffic lights properly synchronized, it is expected that once a vehicle gets a green light it can proceed past many other lights without getting interrupted by a signal that turns red. Given its importance, the research on traffic light control is by no means complete. A number of traffic signal control models have been developed in the past [3–6]. Basically they can be classified by two approaches. The first approach is developed mainly for undersaturated traffic. Vehicles move more or less at the design speed and there is no congestion. The other approach is developed mainly for oversaturated traffic. The queues persist and cannot be cleared totally. The dynamics of queue formation and dissipation becomes critical. Though the proposed procedures do provide rules-of-thumb based on experience, most of them are *ad hoc* in nature. With the transition from undersaturated to oversaturated traffic remaining unclear, it is hard to judge how to switch the operation from one mode to the other, which has a crucial impact on the rush hour traffic in a big city.

The objective of this paper is to study the effects of traffic signal synchronization with a coherent approach applicable to all traffic conditions. It aims at unifying the two different approaches, thus removing the need to switch from one approach to another as traffic is gradually building up or dissipating. This is achieved by taking advantage of a basic traffic model [7,8], which covers the full range of the fundamental diagram. The model is introduced in the following section. The results for undersaturated, oversaturated traffic, and the transition are presented in Secs. III, IV, and V, respectively. Discussions and conclusion are presented in Sec. IV.

II. MODEL

Synchronization effects among a series of traffic signals are studied with a simple configuration of one-way traffic along a single-lane ring. Within the approach of cellular automata, the road is taken as a lattice of 1000 sites, which corresponds to a length of 7.5 km in reality. As the periodic boundary condition is enforced, the vehicular density ρ is a conserved quantity and will be used to specify the underlying dynamics. In the model, each lattice site can be occupied at most by a vehicle. Thus the number of vehicles is an integer in between 0 and 1000, which corresponds to a density from 0 to 1. All the vehicles are subjected to the same driving behaviors, which are prescribed by the well known Nagel-Schreckenberg traffic model [9]. The configuration consists of the position and speed of each vehicle. At each time step, the configuration of vehicles is updated by the following four rules, which are applied in parallel to all vehicles. The first rule is the acceleration. If the speed of a vehicle is lower than v_{max} , the speed is advanced by 1. The second rule is the slowing down due to other vehicles. If a vehicle has d empty sites in front of it and a speed larger than d , speed is reduced to d . The third rule is the randomization, which introduces noise to simulate the stochastic driving behavior. The speed of a moving vehicle ($v \geq 1$) is decreased by 1 with a braking probability p . In the fourth rule, the position of a vehicle is shifted by its speed v . In reality, one time step corresponds to 1 sec. The vehicular behaviors are parametrized by the speed limit v_{max} and stochastic noise p . In city traffic, a setting of $v_{max} = 3$ corresponds to a speed limit of 81 km/h, which provides a reasonable upper limit of speed. As to stochastic noise, a setting of $p = 0.1$ is also expected.

Along the road, ten traffic lights are set up and distributed

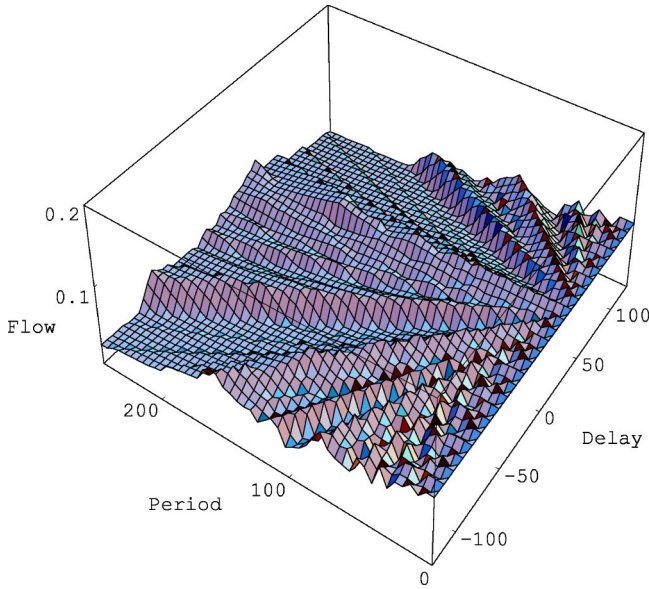


FIG. 1. Traffic flow as a function of signal period and delay at low density $\rho=0.03$, which corresponds to 4 vehicles/km in real traffic. The traffic flow 0.1 corresponds to 360 vehicles/h. Both the signal period and the synchronization delay are measured in seconds.

uniformly. In practice, as vehicles are hopping on the lattice, ten specific links are designated as the traffic lights. The traffic light switches to green and red periodically. In the green phase, vehicles can hop through the link without hindrance. In the red phase, vehicles are not allowed to pass the link and have to stop until the next green phase to pass the link. The operation of a traffic light introduces only localized disturbances to the traffic flow. The effects of anticipation are suppressed, i.e., when the red light is on, the first vehicle stops because the signal switched; while the following vehicles stop because they have to keep a safety headway to the preceding vehicle. The operation of a traffic light is characterized by the signal period T and the ratio α allocated to the green phase [10]. The signal period is understood as the duration of a green phase and a red phase. The signal period T is the basic control parameter of a traffic light. The setting of ratio α reflects the configuration of the intersection. When the crossroad is equitable, $\alpha=0.5$ is expected. When a main road intersects a sideway, $\alpha>0.5$ is assigned to the main road. In this work, we assume all the traffic lights are operated with the same period T and the same $\alpha=0.5$. Furthermore, the synchronization delay δ is introduced to measure the time delay between two nearby traffic lights. Again, the same synchronization delay is applied to all of the nearby traffic lights as their separation is constant. Thus, the operation of these ten traffic lights is characterized by only two parameters: the signal period T and the synchronization delay δ .

III. LOW-DENSITY REGION

When the density is low, vehicles move freely. There are no traffic jams on the road. The traffic lights become the only

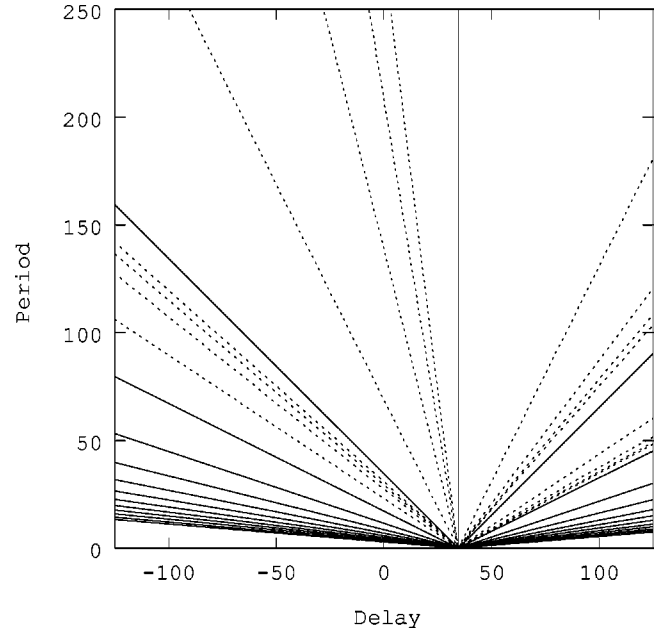


FIG. 2. Maxima of the traffic flow at low density. The primary maxima are shown by the solid lines; the secondary ones by the dashed lines.

hindrance along the journey. The influence of the traffic lights is shown in Fig. 1. By varying the signal period T and the synchronization delay δ , the traffic flow changes significantly. A pattern of a wavelike structure radiating from point $(T, \delta)=(0,34)$ can be clearly observed. Such a traffic pattern reflects that the vehicular speed is constant. When the density is low, the average speed is determined mainly by the imposed speed limit and can be expressed as $\langle v \rangle = v_{max} - p$. With the appropriate delay of $\delta = \Delta L / \langle v \rangle$, vehicles are expected to pass the traffic lights without being stopped, where ΔL denoted the distance between two consecutive traffic lights. As the setting of delay is periodic to the signal period T , such green-light wave solutions can be extended to $\delta + aT = \Delta L / \langle v \rangle$, where a is any integer. The analytic result is shown in Fig. 2, where the locations of the maximum traffic flow are well reproduced. With other settings of T and δ , vehicles are not expected to pass all the traffic lights without being stopped. A cycle of stop-and-go is expected for each vehicle.

With the parametrization $\delta + aT = \Delta L / \langle v \rangle$, delay δ can be replaced by parameter a , i.e., the operation of traffic lights is now specified by parameters T and a . The green-light wave solutions are characterized by integer a . When a assumes a noninteger number, the stop-and-go traffic is realized. Without losing generality, we restrict to the parameter range $a \in (0,1)$ in the following discussion of the stop-and-go cycles. Consider a vehicle passing a traffic light in the beginning of a green phase. The vehicle is expected to pass n green lights before stopped by a red light. At the red light, the vehicle waits a time t for the traffic light to turn green. When the vehicle starts to move again, the situation is then back to our first consideration. After some manipulation, the following analytic expressions can be obtained,

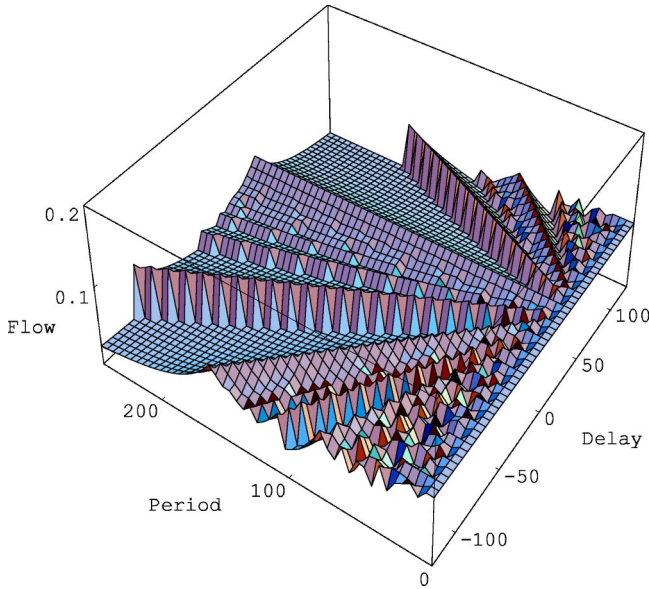


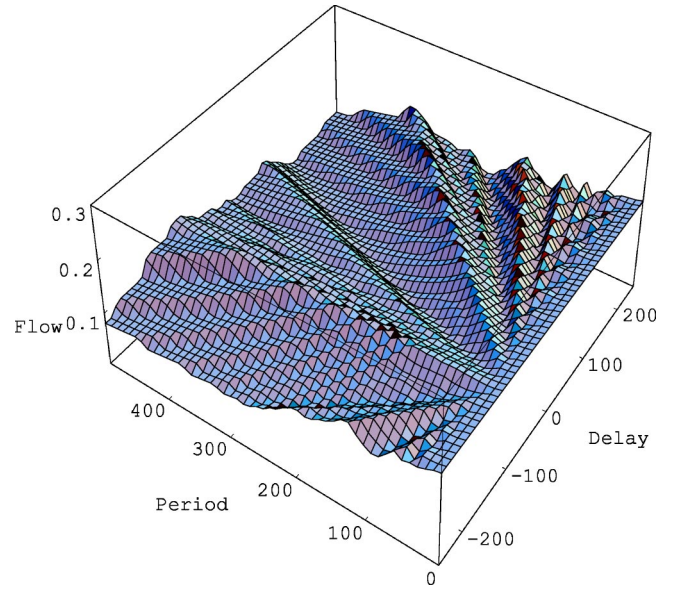
FIG. 3. Analytic results corresponding to Fig. 1.

$$n = \left\lfloor \frac{1}{2a} \right\rfloor, \quad (1)$$

$$t = T - (n + 1)aT, \quad (2)$$

where $[x]$ denotes the step function returning the largest integer less than x . The free-moving time of the vehicle is then $t_0 = (n + 1)\Delta L / \langle v \rangle$. Thus the average speed can be written as $(v_{max} - p) t_0 / (t_0 + t)$ and the traffic flow becomes $\rho(v_{max} - p) t_0 / (t_0 + t)$. The results are shown in Fig. 3. The features observed in the model can be well described. It is interesting to note that the primary maxima of traffic flow can be reproduced by $a = 1$, which implies correctly $t = 0$ from Eq. (2). However, the implication of $n = 0$ from Eq. (1) is erroneous. The vehicles will not encounter any red light. In contrast, setting $a = 0$ reproduces correctly $n \rightarrow \infty$ from Eq. (1), while the resultant traffic flow is erroneous owing to the incorrect implication of $t = T/2$ from Eq. (2). In between the primary maxima, we observe a series of secondary maxima, which can be related to the discontinuity of the step function at $a = 1/(2m)$, where m is an integer. In the special case of $m = 1$, i.e., $a = 1/2$, the maximum flow can also be achieved. It is interesting to note that the traffic flow is continuous around the primary maxima. For $a = 1 \pm \epsilon$, the traffic flow is $\rho(v_{max} - p)(1 - \epsilon T \langle v \rangle / \Delta L)$. While around the secondary maxima, the traffic flow is discontinuous. For example, when parameter a increases from $(1/2) - \epsilon$ to $(1/2) + \epsilon$, the traffic flow drops abruptly by a finite value of $\rho(v_{max} - p)[\Delta L / \langle v \rangle] / [(\Delta L / \langle v \rangle) + (T/2)]$. Thus, along the secondary maximum, the traffic flow is highly unstable to the setting of control parameters.

In summary, the basic pattern of traffic flow can be well understood by considering the behavior of a single vehicle. The pattern is characterized by a single parameter: the average speed of a free-moving vehicle. In the low-density region, the average speed is independent of the vehicular density. As the density varies, the flow is proportional to the


 FIG. 4. The traffic flow at high density; the same as in Fig. 1 with a density $\rho = 0.8$, which corresponds to 107 vehicles/km in real traffic. Both the scales of T and δ are doubled in comparison to Fig. 1.

density and the pattern remains the same as shown in Fig. 1. In practice, such a low-density description can be adapted for $\rho < 0.2$. For $\rho > 0.2$, the average speed deviates significantly from the speed limit. As the traffic jams begin to emerge, much more fluctuations are expected. The average speed alone can no longer provide a fair description of the flow pattern.

IV. HIGH-DENSITY REGION

Next, we consider a high-density region, where the traffic jams become dominant. A typical traffic pattern is shown in Fig. 4. We observe a structure similar to the low-density case. However, the optimal delay becomes negative, i.e., the origin of radiating structure shifts to $(T, \delta) = (0, -111)$. The whole pattern of traffic flow is expected to be characterized by a single speed, which assumes a negative value. Thus the backward moving of the well formed traffic jams becomes the characteristics of the system. The structure can be described analytically as $\delta + aT = -\Delta L / \langle v \rangle$, where $\langle v \rangle = (1 - p)$ denotes the average speed of the backward moving jams. The results are shown in Figs. 5 and 6. The maxima of traffic flow can be well described by $(1 - \rho)(1 - p)$. With further increase in density, the flow decreases accordingly. However, as the speed of the backward moving jams is independent of the vehicular density, the flow pattern shown in Fig. 4 is independent of the density varying. In practice, such a high-density description can be adapted for $\rho > 0.5$. We further note that the characteristic speed in the high-density region is much less than that in the low-density region, i.e., $(1 - p)$ versus $(v_{max} - p)$. Compared to the flow pattern in the low-density region, a similar structure in the high-density region is revealed only when we explore the parameter space (T, δ) to a larger scale. However, a setting of $T > 250$ is not possible in reality.

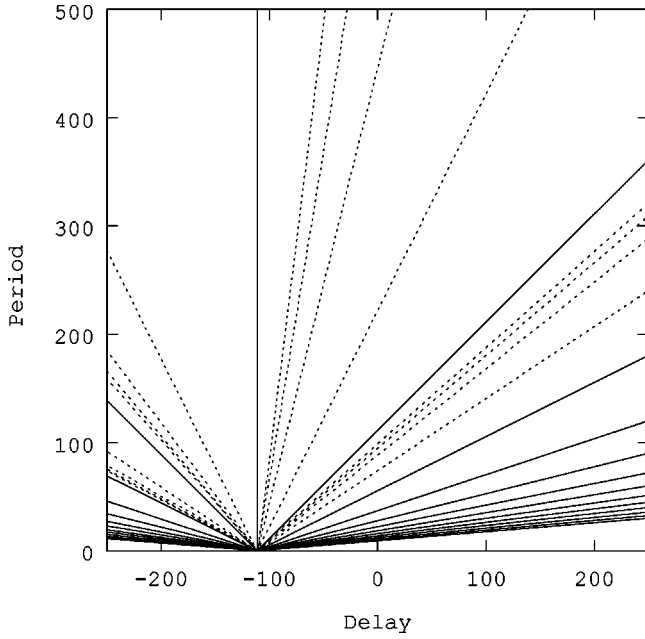


FIG. 5. Maxima of traffic flow at high density; the same as in Fig. 2.

V. INTERMEDIATE-DENSITY REGION

In the transition between low- and high-density regions, the traffic flow is rather insensitive to the variation of various parameters, such as T , δ , and ρ . As long as the signal period is not set too large, the traffic flow is observed to saturate to a constant value. With naive expectation, the saturated flow assumes a fraction α to the maximum flow in a system without traffic lights. The typical results are shown in Fig. 7.

Queues at road intersections will not dissolve completely within one cycle of the green-light phase. Vehicles are caught in stop-and-go cycles. A vehicle just past a traffic light in the green-light phase will usually be trapped by a traffic jam,

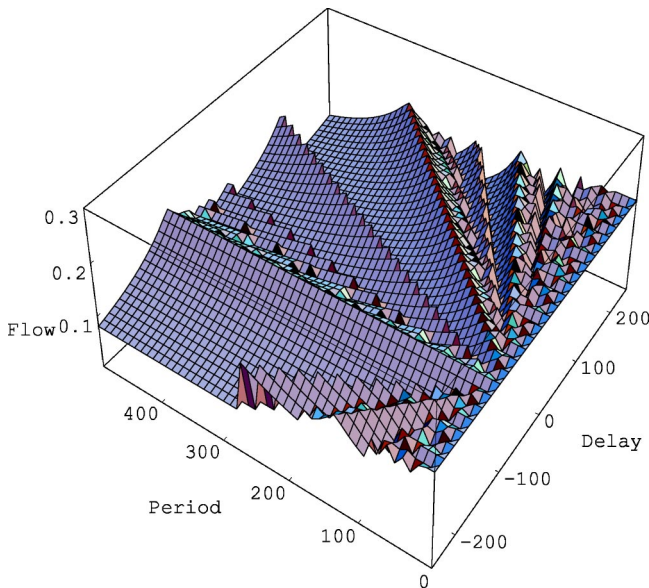


FIG. 6. Analytic results corresponding to Fig. 4.

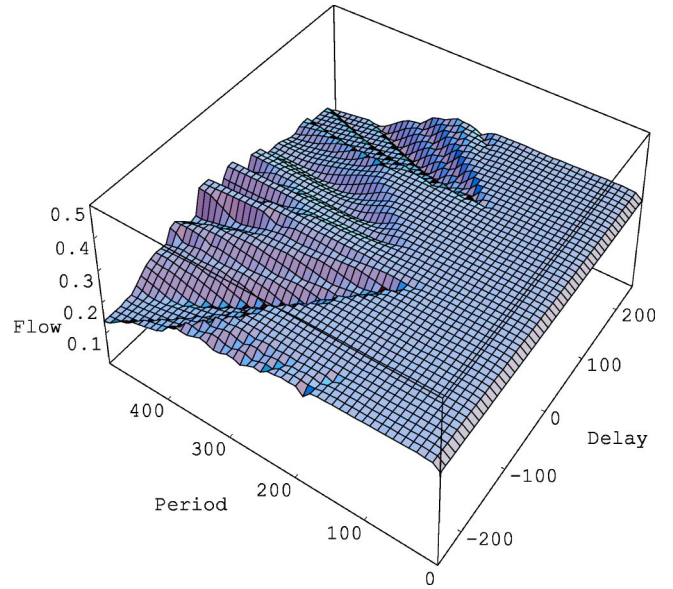


FIG. 7. The traffic flow at the transition region; the same as in Fig. 4 with a density $\rho=0.35$, which corresponds to 47 vehicles/km in real traffic.

which is the undissolved queue from the next traffic light ahead. Only after spending some time in the slow moving within the jam will the vehicle gain speed again and rush to the next traffic light, which is often switched to a red-light phase already. Once in a while, some vehicles might get a chance to pass two consecutive traffic lights smoothly. The spatiotemporal queue dynamics is shown in Fig. 8. Three distinct phases can be observed in the space-time plot: free-flow, jam, and vacancy. In the free-flow, phase vehicles move freely with speed $(v_{max} - p)$; in the jam, the fronts propagate backward with speed $(1 - p)$. Thus the phase boundaries can be characterized by three speeds: $(v_{max} - p)$, $(1 - p)$, and 0. Speed 0 is attributed directly to the traffic stopped by a red light. In contrast, only two phases are observed on the highways with a bottlenecklike toll booth or lane merge, where the traffic is not required to stop completely. When the traffic is interrupted by the red light, the queue and vacancy appear before and after the intersection, respectively. As shown in Fig. 8, the free-flow phase occupies half of the area in the space-time plot, which is a direct manifestation of parameter $\alpha=0.5$. The areas occupied by the other two phases can be estimated by the conservation of vehicle number. Neglecting stochastic noise, the following analytic results can be obtained:

$$A_1 = \alpha, \tag{3}$$

$$A_2 = \rho - \frac{\alpha}{v_{max} + 1}, \tag{4}$$

$$A_3 = 1 - \alpha - \rho + \frac{\alpha}{v_{max} + 1}, \tag{5}$$

where A_1 , A_2 , and A_3 denote the ratios of areas allocated to the free-flow, jam, and vacancy, respectively. The positive-

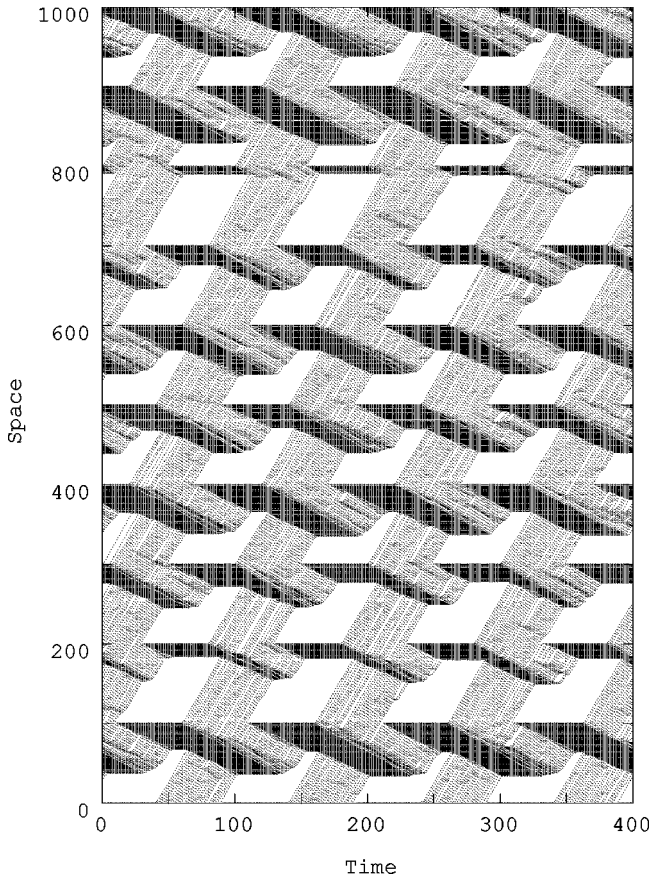


FIG. 8. Space-time plot at the density $\rho=0.35$. The parameters are $T=100$, $\delta=20$, and $\alpha=0.5$. The traffic lights are located at $x=0,100,200, \dots$. The space and time are measured by 7.5 m and 1 sec, respectively.

ness of A_2 and A_3 sets a range of density for the rough estimation. As density increases, the jam extends with the shrinkage of vacancy. In the green-light wave solutions of the low-density region, only the free-flow and vacancy phases are observed; in the high-density region counterpart, only the free-flow and jam phases are observed then.

The basic building block of the spatiotemporal profile is shown in Fig. 9. The queue starts to accumulate once the traffic light switches to red. The queue length increases linearly with time and then saturates when the traffic light in the previous intersection blocks the traffic and the traffic jam in between these two intersections dissolves completely. Once the traffic light switches to green, the queue begins to dissolve. The queue length decreases linearly with time until the vehicles from the previous intersection arrive again. Then the queue keeps a fixed length and moves backward. When the traffic light in the previous intersection blocks the traffic again, the queue dissolves again and disappears completely. With fixed settings of T and δ , the above description can be specified by just one parameter: the saturated queue length l in the red light, see Fig. 9. When l is less than a critical value l_a , the queue dissolves completely before the next wave of vehicles arrive. Thus there is no backward moving queue and most vehicles from the next wave can pass the traffic light

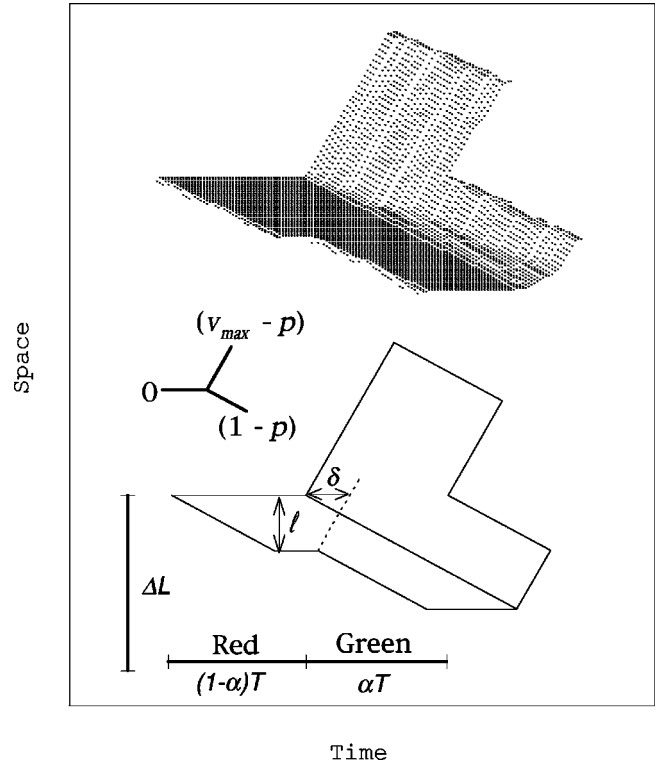


FIG. 9. Building block of the space-time plot shown in Fig. 8.

smoothly. On the other hand, when l is larger than a critical value l_b , the next wave of vehicles arrives before the queue reaches its saturated value. Then the queue profile becomes a wide traffic jam moving backward. The front can be extended backward to a distance l_c from the traffic light. With the simple geometry shown in Fig. 9, the following analytical expressions for these critical lengths can be obtained:

$$l_a = \frac{(v_{max} - p)(1 - p)}{(v_{max} - p) + (1 - p)} \delta, \tag{6}$$

$$l_b = \frac{(v_{max} - p)(1 - p)}{(v_{max} - p) + (1 - p)} (\delta + T - \alpha T), \tag{7}$$

$$l_c = \frac{(v_{max} - p)(1 - p)}{(v_{max} - p) + (1 - p)} (\delta + T), \tag{8}$$

where it is understood that $\delta \in (0, T)$.

As shown in Fig. 8, parameter l can assume different values for different intersections, where the traffic lights are operated with the same T and δ . As time evolves, parameter l at each intersection is basically kept constant. The difference between the queue lengths at each intersection can be retrospectively traced to the initial configuration in the simulations. The average value of l is expected to have a linear dependence on density.

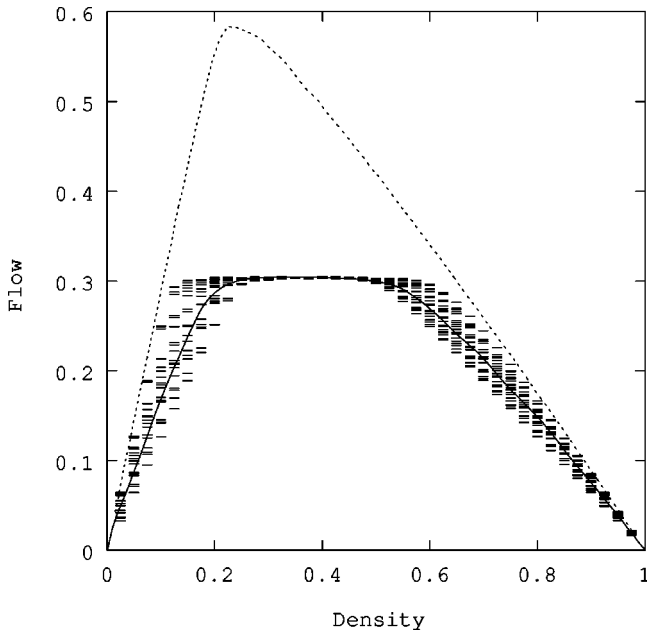


FIG. 10. Fundamental diagram of the model. Data from various settings of δ at $T=100$ are shown. The results of a system without traffic lights are shown by the dashed line. The solid line shows the results when the traffic lights are operated independently. The traffic flow and the vehicular density are measured by 3600 vehicles/h and 133 vehicle/km, respectively.

VI. DISCUSSION

We study the influence of traffic flow due to the synchronization among a series of traffic lights. A simple system consists of a one-lane unidirectional ring road with ten traffic lights distributed uniformly. Both the distances ΔL between two neighboring traffic lights and the ratios α allocated to a green phase are the same for every intersection. Such configuration is ready to be extended to symmetric and regular towns. However, the constancy of ΔL and α is not so restrictive, as simple scaling relations had been observed [10]. The distance ΔL scales with the signal period T , and the ratio α scales with the inverse of vehicular density ρ . As the width of an intersection is neglected in the simulation, unrealistic features in the limit $T \rightarrow 0$ can be noticed. The traffic light becomes an idealized stop sign and the traffic flow can be maintained at the optimal value. However, we would like to emphasize that the benefits of traffic signal synchronization depend heavily on the uniformity of traffic flow. Including the much complicated details would surely reduce the benefits of synchronization. Thus the results from such simplified considerations can be taken as an upper bound to the benefits.

The results can be summarized by the traditional fundamental diagram shown in Fig. 10. The operation of traffic lights at intersections provides a simple time-sharing mechanism to regulate the traffic flow in different directions. In comparison to the system without traffic lights, the maximum flow is then down to a fraction α only. When the density is low, the effects of synchronization are prominent. With appropriate settings of the delay δ , vehicles can pass

the intersections without being stopped by the traffic lights. On the other hand, if the setting is away from one of the optimal values, the traffic flow is largely diminished. From the drivers' experience, whether or not the setting is appropriate can be easily discerned. However, such expectation for green-light waves becomes inaccessible when the density increases. In the intermediate-density region, the traffic flow saturates. The synchronization has no effect to the traffic flow. Traffic jams become inevitable no matter how one adjusts the setting. Interestingly, when the density is large enough, the effects of synchronization begin to manifest again. Like its low-density counterpart, the traffic flow can be maintained at the optimal value by an appropriate setting of the delay δ . The presence of traffic lights will provide no further hindrance to the mobility of vehicles. We note that the appropriateness of the setting should be judged by the uninterrupted backward moving of the jam front. The smooth forward moving of vehicles is already inaccessible. From the drivers' point of view, these optimal settings can be related to the small gap produced when a traffic light switches to red, which provides a measure to the vacancy phase in the space-time plot. The optimal settings of high density are characterized by the disappearance of the vacancy phase.

For one-way traffic, the optimal traffic flow can be maintained by any setting along the primary maxima. When the two-way traffic is considered, further constraints should be imposed to obtain the optimal settings. As the traffic from opposite direction is controlled by the same setting, the results can be deduced from the known results of one-way traffic. For example, in the low-density region, one of the optimal settings can be reached at $T=2\Delta L/\langle v \rangle$ and $\delta = \Delta L/\langle v \rangle$. When the signal period is larger than this value, no optimal setting can be obtained. Alternatively, the optimal setting can also be reached at $T=\Delta L/\langle v \rangle$ and $\delta=0$, where all the traffic lights switch simultaneously.

In this study, stochastic noise in the traffic flow is measured by parameter p . Without noise ($p=0$), the system is deterministic and the exact solution can be obtained analytically. With the noise level of $p=0.1$, uniformity in the traffic is still discernible. The effects of noise can be observed by the variation of traffic flow when the setting is along the primary maximum, see Figs. 1 and 4. As the low-density behavior is mainly controlled by the speed limit v_{max} , increasing the noise level has only minor effects to the results shown in Fig. 1. On the contrary, the high-density behavior is determined mainly by stochastic noise. With noise enhanced, the wavelike structure shown in Fig. 4 is smeared out and the traffic flow becomes independent of both T and δ .

The benefits of synchronization are obvious only when the density is low. From the control scheme point of view, it is important to have a correct estimation of the saturated traffic flow. When the traffic demand surpasses this saturated value, the benefits of synchronization become an illusion. Even if all the traffic lights are operated independently, i.e., with the fixed T but a random delay δ assigned to each traffic light, the throughput remains the same, see Fig. 10. We further note that even in the low-density region, if parameter δ is not set properly, synchronization of traffic lights will result in a throughput less than that of the randomly operated traffic

lights. Although the benefits of synchronization are expected to manifest when the density becomes higher enough, it is not so promising. The real traffic in the high-density region reveals much larger noise. With the effects of slow-to-start

[11] taken into account, the benefits of synchronization can be totally wiped out. No wonder the gridlocks developed more often than not, even if the traffic lights were well synchronized.

-
- [1] For example, TRANSIMS, Transportation Analysis and Simulation System, Los Alamos National Laboratory, U.S. See <http://transims.tsasa.lanl.gov>
- [2] D. Chowdhury, L. Santen, and A. Schadschneider, Phys. Rep. **329**, 199 (2000).
- [3] H. Simao and W. Powell, Transp. Sci. **26**, 296 (1992).
- [4] B. De Schutter and B. De Moor, Eur. J. Control **3**, 260 (1998).
- [5] H.K. Lo, Transp. Res., Part A: Policy Pract. **33**, 433 (1999).
- [6] T.H. Chang and J.T. Lin, Transp. Res., Part B: Methodol. **34**, 471 (2000).
- [7] P.M. Simon and K. Nagel, Phys. Rev. E **58**, 1286 (1998).
- [8] E. Brockfeld, R. Barlovic, A. Schadschneider, and M. Schreckenberg, Phys. Rev. E **64**, 56 132 (2001).
- [9] K. Nagel and M. Schreckenberg, J. Phys. I **2**, 2221 (1992).
- [10] D.W. Huang and W.N. Huang, Int. J. Mod. Phys. C (to be published).
- [11] R. Barlovic, L. Santen, A. Schadschneider, and M. Schreckenberg, Eur. Phys. J. B **5**, 793 (1998).